# End-user evaluation of software-generated intervention planning environment for transrectal magnetic resonance-guided prostate biopsies

Jose D. Velazco-Garcia[1] | Nikhil V. Navkar[2] | Shidin Balakrishnan[2] | Julien Abi-Nahed[2] | Khalid Al-Rumaihi[2] | Adham Darweesh[3] | Abdulla Al-Ansari[2] | Eftychios G. Christoforou[4] | Mansour Karkoub[5] | Ernst L. Leiss[1] | Panagiotis Tsiamyrtzis[6] | Nikolaos V. Tsekos[1]

[1]Department of Computer Science, University of Houston, Houston, Texas, USA

[2]Department of Surgery, Hamad Medical Corporation, Doha, Qatar

[3]Department of Clinical Imaging, Hamad Medical Corporation, Doha, Qatar

[4]Department of Mechanical and Manufacturing Engineering, University of Cyprus, Nicosia, Cyprus

[5]Department of Mechanical Engineering, Texas A&M University—Qatar, Doha, Qatar

[6]Department of Mechanical Engineering, Politecnico di Milano, Milan, Italy

**Correspondence**
Jose D. Velazco-Garcia, MRI Lab, Department of Computer Science, University of Houston, 4800 Calhoun Road PGH 501, Houston, TX, USA.
Email: jdvelazcogarca@uh.edu

**Funding information**
Division of Graduate Education, Grant/Award Numbers: 1433817, 1746046; Division of Computer and Network Systems, Grant/Award Number: 1646566; Qatar National Research Fund, Grant/Award Number: 9-300-2-132

## Abstract

**Background:** This study presents user evaluation studies to assess the effect of information rendered by an interventional planning software on the operator's ability to plan transrectal magnetic resonance (MR)-guided prostate biopsies using actuated robotic manipulators.

**Methods:** An intervention planning software was developed based on the clinical workflow followed for MR-guided transrectal prostate biopsies. The software was designed to interface with a generic virtual manipulator and simulate an intervention environment using 2D and 3D scenes. User studies were conducted with urologists using the developed software to plan virtual biopsies.

**Results:** User studies demonstrated that urologists with prior experience in using 3D software completed the planning less time. 3D scenes were required to control all degrees-of-freedom of the manipulator, while 2D scenes were sufficient for planar motion of the manipulator.

**Conclusions:** The study provides insights on using 2D versus 3D environment from a urologist's perspective for different operational modes of MR-guided prostate biopsy systems.

**KEYWORDS**
MRI-guided interventions, transrectal prostate biopsy, 2D/3D visualizations

## 1 | INTRODUCTION

Prostate cancer is the most common non-skin malignancy affecting men globally.[1] The prostate-specific antigen (PSA) test and digital rectal examination (DRE) are the primary tools for screening for prostate cancer.[2,3] Prostate cancer is generally suspected in patients with an elevated PSA or abnormal DRE. However, a positive screening test is not indicative of malignancy and needs to be further evaluated histologically through biopsy sampling of the prostate, prior to initiating any treatment protocols.[4]

In most cases, the biopsy method involves an 18-guage spring-loaded core biopsy needle inserted manually into the prostate via a transrectal probe. The probe can be operated in either Mode-I or Mode-II, as shown in Figure 1A. Mode-I enables side-firing of the needle, entering the prostate at an angle from the side of the probe,

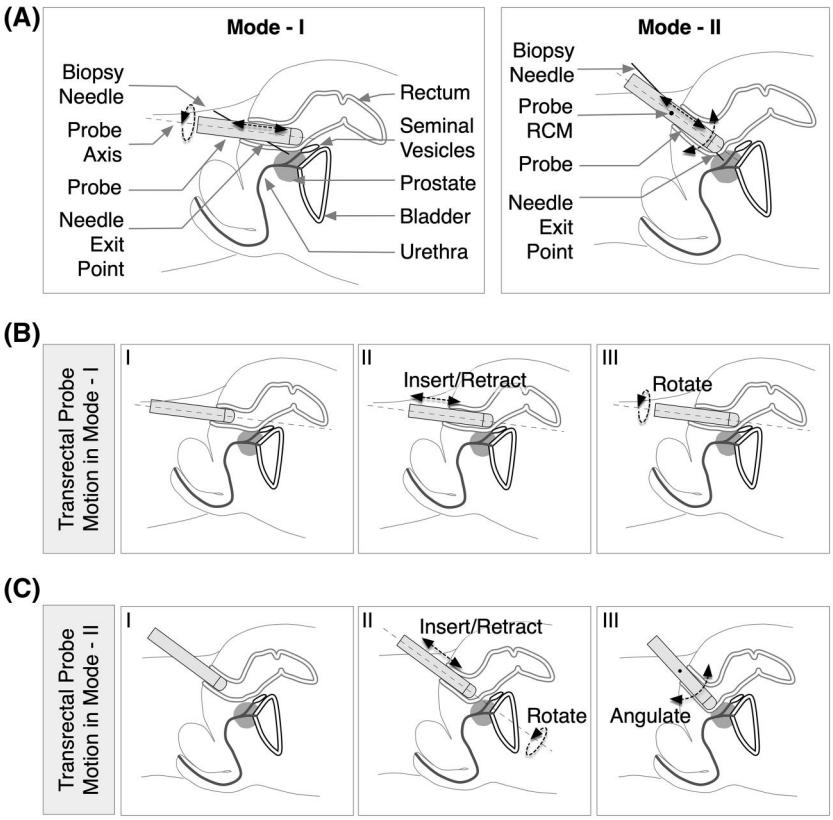


**FIGURE 1** (A) Illustration of the two modes of operation for magnetic resonance-guided transrectal prostate biopsy. The modes are based on motion of the probe inside the rectum to target different regions of the prostate. (B) In Mode-I, the probe is inserted in the rectum (B-I) and then the manipulator is actuated to insert/retract (B-II) or rotate (B-III) the probe along the probe axis to target the lesion in the prostate. The probe axis is shown as a dotted line. (C) In Mode-II, the probe is inserted in the rectum (C-I) and then the manipulator is actuated to either insert/retract or rotate the probe along the probe axis (C-II) or angulate it (C-III) around an remote center of motion (RCM) to target the prostate lesion. The probe axis is shown as a dotted line, whereas the RCM is shown as dot

and includes translation and rotation motions along a virtual axis inside the rectum (as shown in Figure 1B). Similarly, Mode-II enables end-firing of the needle, where the needle enters the prostate from the distal tip of the probe. It includes additional upward and downward angulation using the anus as a fulcrum (as shown in Figure 1C). The trajectory of the chosen needle-exit directly affects patient positioning, surgical technique, probe movements to obtain the biopsy and cancer detection rates.[5,6] Theoretically, both modes provide good visualization under optimal conditions and patient positioning; in many institutions, it boils down to surgeon-preference and experience. The end-firing probe allows for better lateral-visualization of the prostate and has better cancer-detection rates.[5,6] It also provides easier access to, and biopsy of, the lateral and anterior regions of the prostatic peripheral zone as well as apex of the prostate.[5,6] This further lowers the risk of a false-negative biopsy. However, the end-firing probe (Mode-II) is highly dependent on patient-positioning (glutes on the edge of the bed with legs flexed to the chest, to allow for probe movement upward and downward using anus as fulcrum), while side-firing probes (Mode-I) are relatively position-independent (as long as the anus is accessible). Because of their better patient-tolerance profile, many experienced urologists prefer side-firing probes (Mode-I) for prostate biopsies.[7,8] To an experienced urologist, there is no significant difference in cancer-detection for either mode.[9] In contrast, with a novice urologist, the mode directly affects patient positioning, probe movements, and, most significantly, cancer detection rates.[5,6]

Apart from the two modes, depending upon the imaging modalities, the standard approaches for prostate biopsies can be categorized into transrectal ultrasound guided, magnetic resonance (MR)-guided and MR-ultrasound fusion.[10] This study focuses on MR-guided biopsies of the prostate using an actuated manipulator to control a transrectal probe under the two modes of operation. MR-guided biopsies require MR-compatible instruments, prolonged positioning of patient in prone position within the MRI and extended occupation of usage-slots of MR machines. Despite these requirements, it is the most sensitive modality to accurately detect and sample prostate lesions.[11,12] The manipulator provides precise positioning of the probe inside the rectum, improving the accuracy of the procedure.[13–19]

An interventional planning software acts as a human-machine-interface between the operator and the actuated biopsy system. It enables the visualization of the area of interest for biopsy-planning. Thus, the accuracy of the procedure is affected by the operator's ability to understand the intervention environment rendered by the software and plan the intervention by actuating the virtual manipulator. Based on this concept, this study presents a user-study to evaluate the operator's interaction with an interventional planning software and its effects on planning transrectal MR-guided prostate biopsies.

There have been studies that have assessed software for transrectal MR-guided prostate biopsies. Some of these studies focus on the evaluation of the used software in terms of the accuracy of the procedure performed on subjects,[20] whereas others report their results on MR-ultrasound fusion accuracy[21] and accuracy of the biopsy needed with respect to the collected MR images.[22] Other studies evaluate the software used in conjunction with a manipulator to assess calibration and registration of the manipulator and the virtual environment[23] as well as to assess the feasibility to remotely control the manipulator.[18] Although these studies provide meaningful insight for MR-guided transrectal prostate biopsies, they do not provide a user (urologist) evaluation in terms of intuitiveness and interactivity of the biopsy planning environment in 3D and 2D. In this study, we report results from studies conducted with urologists with different levels of expertise to evaluate their performance when controlling a virtual manipulator to plan MR-guided transrectal prostate biopsies under different modes of operation and visualization.

## 2 | MATERIALS AND METHODS

### 2.1 | Design of software based on clinical workflow

A generic software was developed taking into consideration the regular clinical workflow followed at hospitals for performing transrectal MR-guided prostate biopsies. The steps for this workflow, as shown in Figure 2, can be broadly categorized into five phases: pre-procedure, imaging, planning, intervention and post-procedure. After the pre-procedure phase, the interlinked steps of imaging, planning and intervention phases are executed using the software. MR images acquired in the imaging phase are used in the planning phase for registration and planning of the biopsy needle trajectory. The manipulator and probe have fiducial markers, which are identified from the MR images and used to co-register physical entities (i.e., the manipulator and probe) with their virtual representations. In the planning environment, two probes are rendered. First, a virtual probe that reflects the actual pose of the physical probe. The pose of the virtual probe is altered in the software only when the physical probe moves. Second, the virtual probe's proxy, which is a replica of the virtual probe. Unlike the virtual probe, the pose of the virtual probe's proxy can be manipulated by the operator in the software and is used to simulate the manipulation of the probe required for planning the biopsy needle trajectory. The operator analyzes the acquired MR images to visualize the intervention region and adjust the pose of the virtual probe's proxy, so that the biopsy needle can hit the targeted lesion. Once the virtual probe's proxy is in the correct pose (as required by the operator), the software sends actuation commands to the physical manipulator which positions the physical probe inside the patient's rectum. The pose of the virtual probe is then re-registered based on the new location of the physical probe. If the biopsy can be performed successfully, a needle is manually inserted to extract the tissue sample. To get new samples, or if the physical probe is not in the correct pose, the virtual probe's proxy is repositioned, and the above steps are re-executed.

### 2.2 | Development of the interventional planning software

A software adhering to the clinical workflow (as shown in Figure 3) was developed.[24,25] The software is a modular system with the following functionalities: (a) positioning/rendering of virtual objects (such as MR images, probe and manipulator) in 2D and 3D scenes, (b) manipulation of 2D/3D scenes (via rotation, panning and zooming) to analyse the area of intervention from different perspectives, (c) processing of operator input through a graphical user interface (GUI), (d) built-in controls for the virtual manipulator/probe and (e) textual feedback for the operator on system events, such as information on loaded data, warnings and confirmation of planning parameters. The modules were developed in C++ and integrated based on a previous computational platform.[26] The GUI was implemented using the Qt framework,[27] and the visualization was performed using the Visualization ToolKit library.[28] The characteristics of the virtual objects rendered in the 2D/3D scenes are described as follows:

- *MR scanner and images*: A cylindrical MR scanner bore and a movable rectangular bed inside the bore are rendered in the 3D scene. MR images are rendered in both 2D and 3D scenes. The scene's windows have GUI elements to traverse through the slices, change the selected slice orientation (coronal, sagittal and transverse), and load more slices of MR images. Interaction with slices through the GUI is reflected on both 2D and 3D scenes. The 2D scene window also displays coordinates of the image voxel corresponding to the cursor position over the slice.
- *Manipulator*: A virtual manipulator was designed based on the movements exhibited by existing transrectal prostate biopsy systems[15–17,19] and is placed on the MR scanner bed in the 3D scene. The generic design of the manipulator is comprised of three links (base, support arm and distal arm) with two rotational degrees-of-freedom. The distal arm comprises: (a) an adapter to connect different probe designs and (b) a mechanism to rotate and translate the connected probes, thus providing two additional degrees-of-freedom. Therefore, the manipulator, along with a probe, offers four degrees-of-freedom: three rotations and one translation. The actuation of these four degrees-of-freedom assists the operator in placing the probe in the required pose, aligned with the targeted lesions in the prostate. In Mode-I, only the probe is actuated by the manipulator, whereas in Mode-II, both the manipulator and probe get actuated. The user can select either mode and actuate each degree-of-freedom individually using the GUI.
- *Probe*: A virtual probe was designed to be operated in both modes and is rendered along with its trajectory of the biopsy needle (in the form of a line) in both 2D and 3D scenes. To assess if the

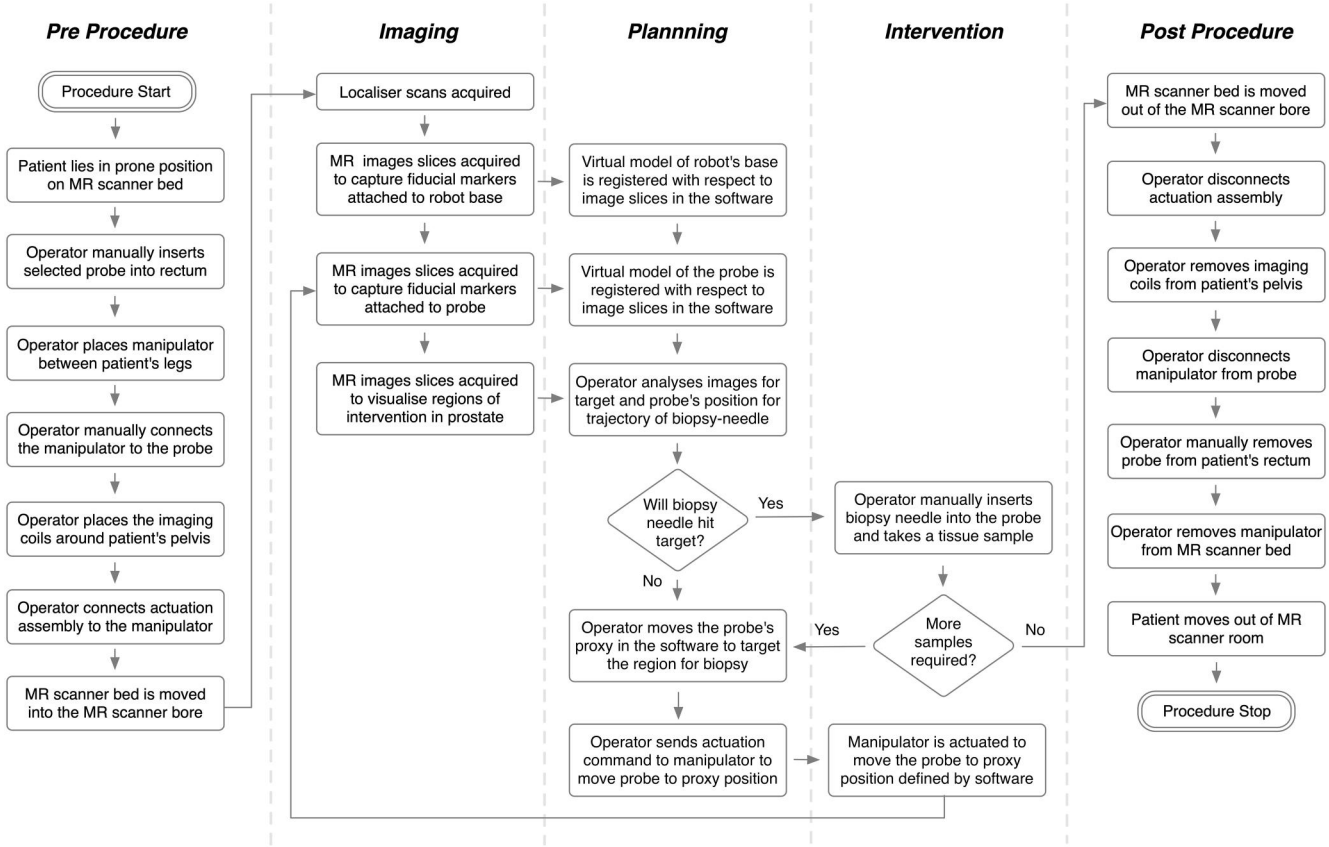


**FIGURE 2** Clinical workflow followed at a hospital to perform magnetic resonance-guided transrectal prostate biopsy using the interventional planning software. The steps of the workflow are sectioned into five phases: pre-procedure, imaging, planning, intervention and post-procedure

current configuration of the manipulator and probe can target a lesion, the probe's workspace is rendered as a span of lines, representing the biopsy needle's potential trajectories in the 3D scene. If the lesion lies outside the workspace, the biopsy is not possible under Mode-I and would require actuation of the manipulator under Mode-II to reach the target.

- *Probe's proxy*: A proxy of the virtual probe was rendered in the 2D scene (as a projection on the MR slices) and 3D scene. During manipulation, the operator visually inspects possible poses to ensure the probe always stays in the rectum and is pressed against the surface of the prostate. Secondly, the software computes feasible poses based on the kinematic constraints imposed by the manipulator and informs the operator.

To simulate the clinical workflow with the developed software, the following assumptions were made: (a) the co-registration of the physical manipulator and probe with their virtual representations is accurate and will be performed by another sub-module, (b) pre-acquired offline MR datasets in DICOM format are used as real-time images, (c) the MR images used are from a prostate phantom and depict the pelvic anatomies and (d) the manipulator, when actuated, reaches the desired pose inside the rectum without any tissue deformations. The images were acquired from an MR compatible prostate phantom (Model 048A; CIRS Inc) on a Siemens 3T Skyra scanner with a T2 Turbo-Spin-Echo (TE: 101; TR: 3600; FS: 3; FOV: 200 × 200 mm; 320 × 320; Slice Thickness: 3 mm; Slice Spacing: 3.3 mm).

## 2.3 | Experimental setup for user studies

The developed software was evaluated for planning transrectal prostate biopsies using a virtual manipulator and MR images acquired from a prostate phantom. Virtual studies were performed due to lack of an available manipulator for experimental studies, as well as to address the challenging logistics of coordinating availabilities of clinicians and physical systems. Usability studies were conducted with eight urologists. The subjects were denoted as $S_i$ (where $i = 1$ to 8) and were categorized based on: (a) professional experience related to urology (Juniors—$S_1$ to $S_6$ were urology residents with less than 5 years of experience, and seniors—$S_7$ and $S_8$ were urology consultants with more than 5 years of experience) and (b) prior experience working with computer generated 3D environment ($S_4$, $S_5$ and $S_6$ had prior 3D environment experience, whereas $S_1$, $S_2$, $S_3$, $S_7$ and $S_8$ had no prior experience).

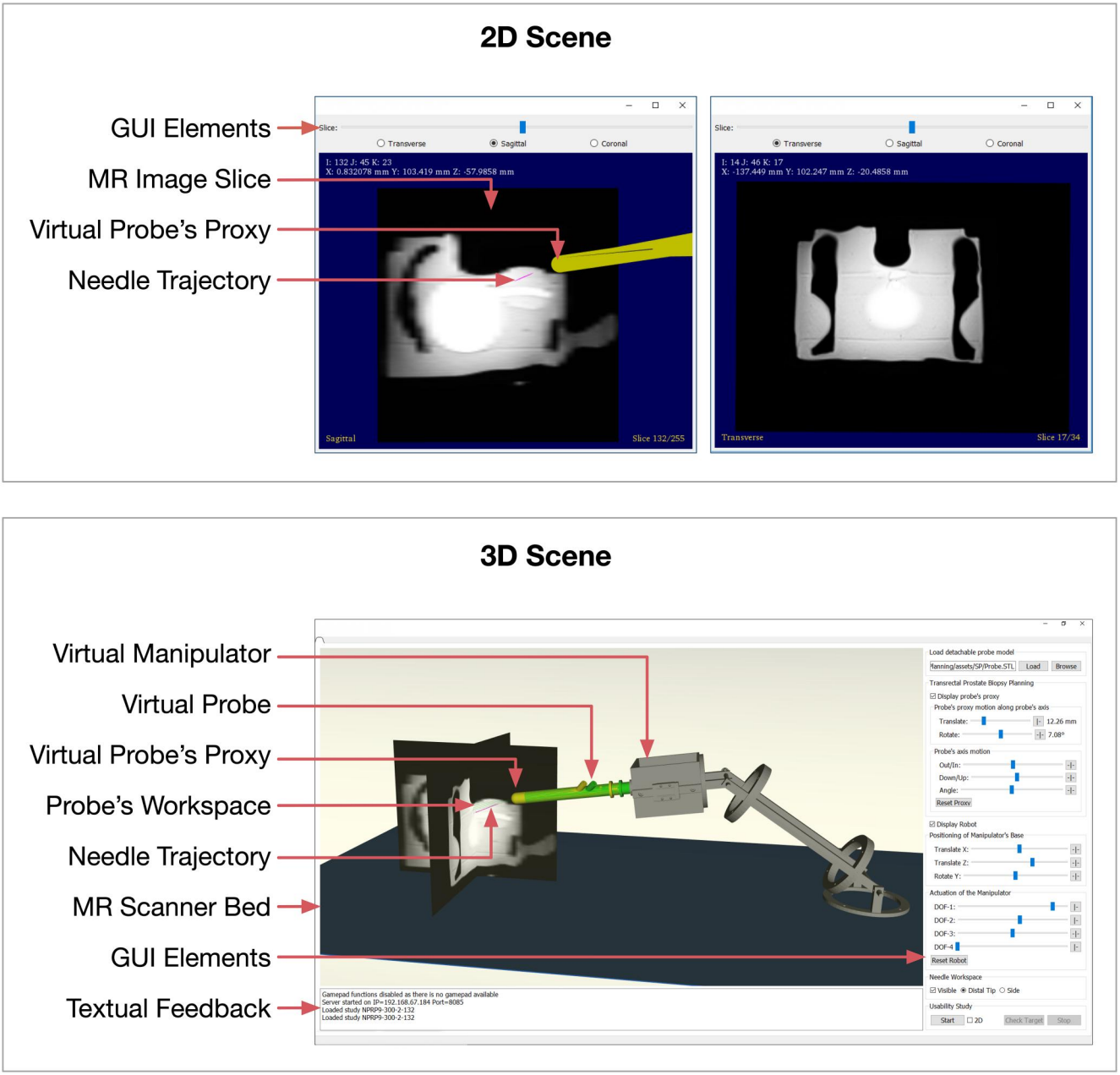


**FIGURE 3** Virtual objects corresponding to the region of intervention rendered by software in 2D and 3D scenes

The software was evaluated by the subjects under (a) Mode-I and Mode-II based on the number of virtual manipulator actuations and (b) two visualization modes (2D and 3D) based on the dimension of the visual information perceived by the operator. The combination of control and visualization modes resulted in four modes of operating of the software, namely Mode-I-2D, Mode-I-3D, Mode-II-2D and Mode-II-3D. For each mode of operation, five spherical targets (with diameters of 4, 5, 2.4, 2 and 1.5 mm, in that order) were pre-placed inside the prostate. The positions of these biopsy targets varied for Mode-I versus Mode-II as different regions of prostate are targeted under the two modes.

In the user studies, the subjects were first introduced to the software through a 30-min preparatory session that included familiarization with the controls of the virtual manipulator/probe through the GUI. Subsequently, subjects were asked to maneuver the probe's proxy connected to the virtual manipulator under different modes of operation until the biopsy was performed successfully. In the virtual environment, a prostate biopsy is considered successful when the subject clicks on the "Check Target" button, and the distance between the biopsy needle and the centre of the target is at most the sum of the target's and needle's radii (0.3 mm).[29] On a successful biopsy, a new target is rendered, otherwise the subject is prompted to continue planning on the existing target. The study is completed when a successful biopsy is performed for all five targets.

During the study, interaction of the subjects with the software was recorded. Meaningful indices were calculated from recorded

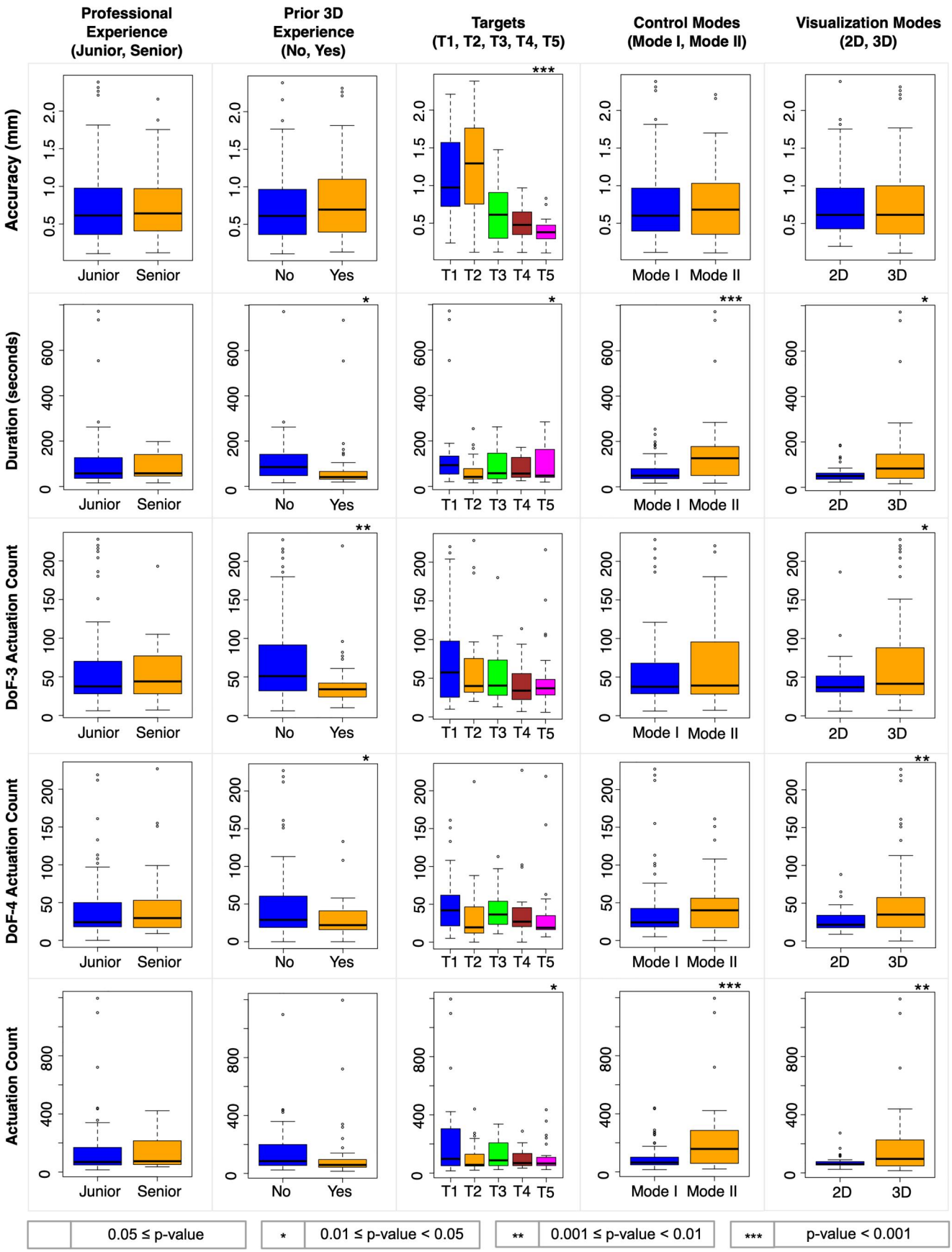
Professional Experience (Junior, Senior)
Prior 3D Experience (No, Yes)
Targets (T1, T2, T3, T4, T5)
Control Modes (Mode I, Mode II)
Visualization Modes (2D, 3D)
Accuracy (mm)
Duration (seconds)
DoF-3 Actuation Count
DoF-4 Actuation Count
Actuation Count
Junior Senior
No Yes
T1 T2 T3 T4 T5
Mode I Mode II
2D 3D
0.05 ≤ p-value
* 0.01 ≤ p-value < 0.05
** 0.001 ≤ p-value < 0.01
*** p-value < 0.001

data related to the performance of subjects when planning transrectal prostate biopsies using the software under different modes of operation. Specifically, for every subject under each mode of operation after performing a successful biopsy on every rendered target, the following values were calculated: (a) accuracy (distance between the centre of the target to the biopsy needle), (b) duration (time required by a subject to perform a successful biopsy on a particular target), (c) actuation count of each degree-of-freedom of the virtual manipulator, (d) total actuation count for all degrees-of-freedom of the virtual manipulator and (e) biopsy missed count (number of times the user clicked on "Check Target" button, but the biopsy needle was not penetrating the target). While performing the studies, it was observed that most of the subjects were not able to operate the software in Mode-II-2D and hence the corresponding values were not reported in these studies.

## 3 | RESULTS

The parameters of the setup comprising professional experience, prior 3D experience, target sizes, control modes and visualization modes constituted the explanatory variables. The logged parameters that describe the state of intervention planning software during user interaction formed the response variables. The response variables consist of accuracy, duration, DoF-3 actuation count (corresponding to rotational degree-of-freedom of the virtual probe attached to virtual manipulator), DoF-4 actuation count (corresponding to translational degree-of-freedom of the virtual probe attached to the virtual manipulator) and total actuation count. Marginal bivariate relationships among response and explanatory variables are visually presented in Figure 4. Statistical modelling was performed to determine which of the explanatory variables of the study were statistically significant in determining each of the response variables. Since the response variables were evaluated on eight distinct subjects, we expect to have some variation coming in the design by the different subjects. For this reason, mixed effect modelling was used allowing to encounter the significant subject to subject variation. The explanatory variables of the study formed the fixed effects whereas subjects were the random effects. In the linear mixed effects model, each of the response variables was transformed, so that we do not get any violation on the basic parametric modelling assumptions (i.e., normality, homoscedasticity, etc.) judged on various diagnostics (like normal probability plots for the residuals, plot of residuals vs. the fitted values, etc.). For each transformed response, $p$-values of the explanatory variables (fixed effects) in the full model were computed. Pairwise relationship among the response variables revealed a correlation of 0.948 between the actuation count and duration, and of 0.727 and 0.684 between total actuation count and DoF-3 and DoF-4 actuation count, respectively.

After performing the statistical analysis, the following observations were made:

- *Subjects' expertise:* Professional experience of the subjects did not show any statistically significant difference in operating the software. However, subjects with prior experience working in computer generated 3D environments took relatively less time to plan a biopsy as compared to the rest of the subjects which had no prior experience ($p = 0.0489$). The average duration per subject with prior 3D experience was 79.5 s as compared to 108.5 s with no experience (shown in Table 1).
- *Targets:* All the subjects were able to perform the biopsies successfully on the rendered targets. The durations to perform successful biopsies for the rendered targets were significantly different among the subjects ($p < 0.0001$). The pattern showed that after two targets the subject got familiar with the intervention planning software; the accuracy and speed improved ($p = 0.0106$).
- *Mode-I* versus *Mode-II:* In Mode-I, subjects took less time to plan and perform biopsies using the virtual manipulator, compared to Mode-II ($p < 0.0001$). In Mode-I, the average duration per subject was 68.5 s, whereas in Mode-II it was 156 s. The average actuation counts for Mode-I and Mode-II were 95 and 222, respectively (shown in Table 2). It showed that Mode-I actuation count was less as compared to Mode-II ($p < 0.0001$).
- *2D* versus *3D visualization modes:* The subjects were able to estimate the insertion length (i.e., the DoF-4) easier in 2D visualization mode as compared to 3D visualization mode ($p = 0.0316$). Also, there were zero target misses in 2D visualization mode.

## 4 | DISCUSSION

Based on these results, a subject's prior experience in using 3D software played a pivotal role in improving the accuracy and time to plan biopsies. There was no indication that a urologist's clinical experience plays a significant role when using the software. Thus, training an operator to work in a computer-generated 3D environment may (a) improve the understanding of the virtually rendered region of intervention, (b) assist in manipulation of virtual objects, which in turn may actuate a manipulator/probe inside the rectum and (c) improve accuracy and speed for performing procedures using the biopsy systems.

Furthermore, familiarity with 3D environments becomes vital when planning and performing an intervention in a 3D scene. For example, in Mode-II-2D, which entailed actuation of all four degrees-

**FIGURE 4** Visualization of the marginal bivariate relationship between the response variables and explanatory variables. The response variables comprise accuracy, duration, DoF-3 actuation count (corresponding to rotation of the probe), DoF-4 (corresponding to translation of the probe) and total actuation count. The explanatory variables consist of professional experience, prior 3D experience, targets, control modes and visualization modes. Each relationship is tagged based on the $p$-value using a star-type categorization: "***" if $p$-value $\leq 0.001$, "**" if $p$-value in (0.001,0.01), "*" if $p$-value in (0.01, 0.05) and " " if $p$-value $> 0.05$

**TABLE 1** Subjects prior experience working in a 3D environment

| | With Prior 3D experience | Without Prior 3D experience |
|---|---|---|
| Average duration (seconds) per subject | 79.5 | 108.5 |
| Average actuations count per subject | 120 | 147 |

**TABLE 2** Modes of operation during the biopsy

| | Mode I | Mode II |
|---|---|---|
| Average duration (seconds) per subject | 68.5 | 156 |
| Average actuations count per subject | 95 | 222 |

of-freedom, subjects were not able to assess the position of the manipulator in 2D and, as a consequence, were not able to perform the studies in an intuitive and timely manner. This necessitates using 3D scenes for an interventional environment when the employed degrees-of-freedom cause a non-planar motion of the device (as in Mode-II-3D). However, contrary to this, subjects may be able to assess motion caused by a single degree-of-freedom better on a 2D scene. For example, during the studies, subjects were able to estimate the insertion length easily on a 2D scene as compared to 3D. Therefore, acquiring and rendering the interventional environment in 2D or 3D scenes assists operators in actuating single or multiple degrees-of-freedom of the manipulator/probe, respectively. Since the number of degrees-of-freedom relates to the dexterity of the device, this conclusion may need to be considered when such devices are implemented.

This study was motivated by the current practice of urologists to view MRI data in a 2D format due to console frontend limitations and lack of intuitive and ergonomic interactive manipulation of 3D imaging data to appreciate and understand the spatial relationships. In response, this study investigated 2D versus 3D visualization and does not compare the specific software platform to any other. It is noted that the features of the custom-developed software can be tuned to be operated as both a standalone software online with the scanner and as a module installed on the scanner computer generating 3D scenes streamed into the console output.

As these studies were conducted in a simulated environment in the absence of an MR scanner and physical manipulator, it had certain shortcomings. First, the study did not include any co-registration of physical objects (manipulator and probe) with their virtual representations. Although this step is crucial in the clinical workflow, the results of these studies were not affected, as it is performed prior to planning.

Second, offline image data were used instead of being online with the MR scanner and accessing the data in real-time or on demand. This limitation also did not affect the user studies that were focused on the interface itself, for two reasons: (i) the difference with being online would have been possible latency in accessing this data that was not included in the studied parameters, (ii) the exact pose of the imaging planes (orientation and position in space) was extracted by the corresponding routine of the software from the DICOM header of the individual slice.

Third, the imaging data used to conduct the studies were acquired from an MR-compatible phantom designed specifically for image-guided prostate biopsy training. Although the phantom does not entirely represent the human physiology of the pelvic region, the anatomies (prostate, urethra, bladder and rectum) necessary for planning the biopsy were of realistic sizes and have similar contrast of MR image data. The structure of the phantom is comprising an orifice leading to a semi-rigid tubular section representing a rectum, which appears as a hollow tube on the MR images. It enabled the user to visualize the virtual transrectal probe motion as if constrained by the rectal walls and improved the user-experience. This would have been difficult with human MR image data unless a probe was inserted in the rectum while acquiring the images.

Fourth, as needle insertion is performed manually by the operator (and thus cannot be simulated in this study), the parameter corresponding to the computation of the needle insertion depth in the software was excluded. The needle insertion depth is equal to the summation of distances traversed by the biopsy needle inside (i) the needle guide of the probe and (ii) in the tissue to target the lesion. The distance traversed inside the probe's needle guide is fixed for Mode-I and Mode-II and is dependent upon the design of the probe used during biopsy. Whereas inside the tissue, the distance traversed by the biopsy needle along the planned trajectory is computed from the point the needle exits the probe till the slit of the biopsy needle (on which the cutting cannula slides) covers the targeted lesion. The slits enable collection of samples <10 mm in length, and the needle has markings at regular intervals that assist the operator to visually measure the distance on the needle and manually insert it into the probe. While inserting the needle in the tissue, deflection of the needle cannot be avoided but can be reduced by following certain approaches.[30] Stone et al. achieved no deflection in 2–6 cm of biopsy tissue length on a phantom by using a 3-point trocar tip on the needle with a 20° vet tip on the cutting cannula.[31] Another potential approach, though demonstrated in transperineal prostate interventions, involves a robot controlling the pose of the needle guide, and the needle is continuously sensed[32,33] and steered[34] while being inserted to minimize the deflection.

Lastly, a prostate biopsy must consider tissue deformation as the probe is being maneuvered inside the rectum. This aspect was not tested in these studies. However, we believe tissue deformation can be addressed by acquiring a new set of real-time MR images after every step when the operator actuates the manipulator/probe and propagating the landmarks from the previous step using computational methods. As shown in Figure 5, the operator moves the probe's proxy in the software to target the region for a biopsy and then sends an actuation command to the manipulator to move the probe to the proxy position. The manipulator is actuated which moves the physical probe.

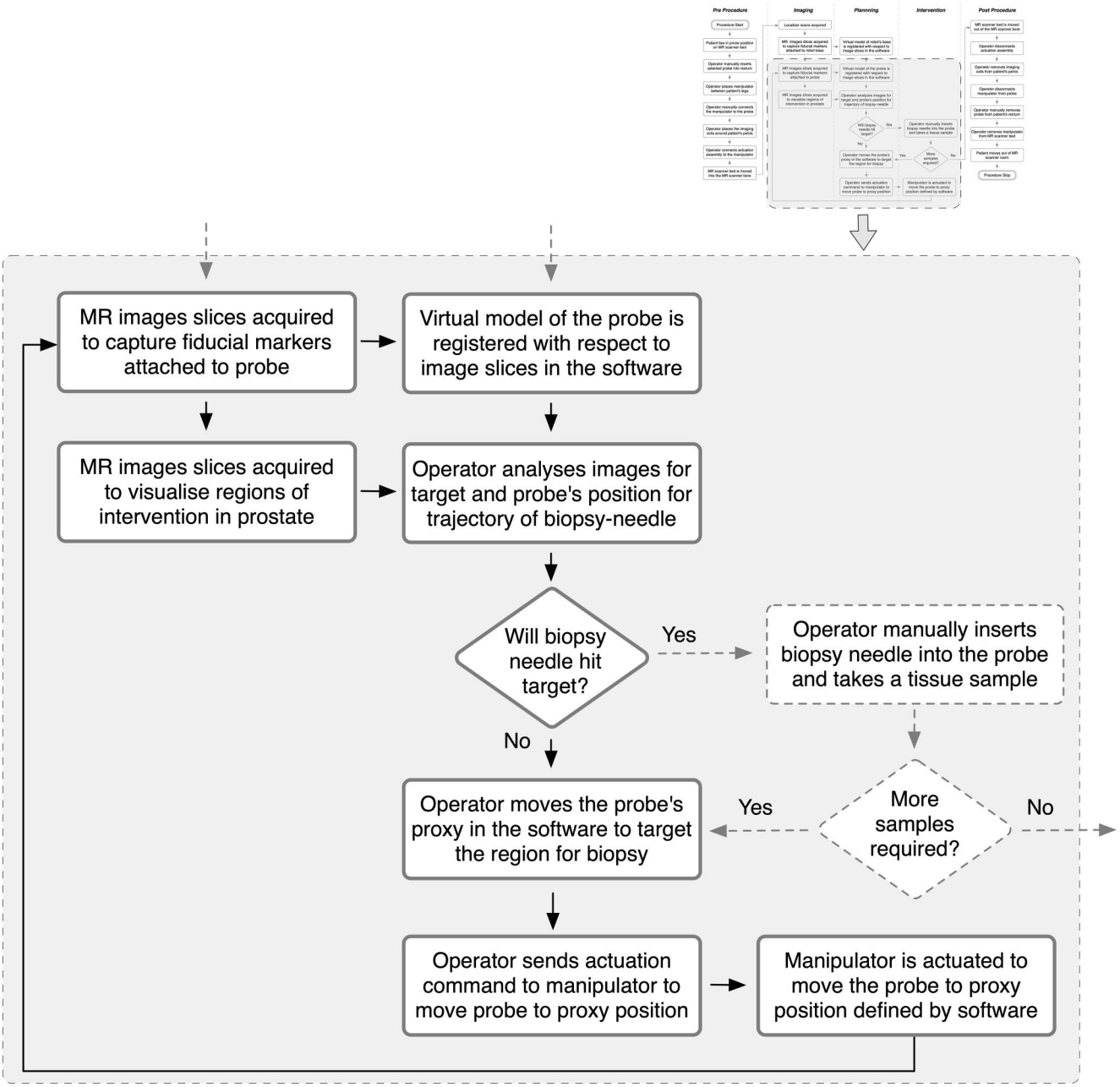


**FIGURE 5** Imaging, planning and intervention steps of the clinical workflow creates a loop that allows the operator to assess the tissue deformation before performing a biopsy

Then, a new set of images are reacquired, depicting the true pose of the physical probe in the software. In the newly acquired set of images, any tissue deformation caused by the motion of the probe or patient movement can be observed by the operator. It should be noted that after manipulation of the probe, the targets identified during the initial planning stage on the MR images need to be propagated in subsequent stages onto the newly collected MR images. This could be achieved by incorporating non-rigid registration algorithms in the software. These image registration algorithms are based on computational approaches that use non-linear warping,[35] b-spline mapping,[36] mutual information registration[37,38] and finite element models.[39,40] The operator re-analyses the biopsy-needle trajectory on these images using the software, and if the biopsy needle will hit the target, the operator manually inserts the biopsy needle into the probe and takes a tissue sample. Otherwise, the operator again moves the probe's proxy in the software (which is reset to the current pose of the physical probe) to target the region for biopsy. This creates a loop which allows the operator to assess the tissue deformation before performing a biopsy. It should be noted that during the step when an operator manually inserts the biopsy needle for tissue sampling, tissue deformation may occur by needle insertion and biopsy gun firing. Studies have shown that biopsy samples can still be obtained for tumors with minimum radius of 2.1 mm with 95% confidence under the assumption of zero error elsewhere in the biopsy system.[41]

Among the metrics used to compare 2D versus 3D interfaces was the accuracy of the virtual biopsy in the computer-generated environment. These results were important in quantifying user performance and assessing the relative value of the two interfaces in those specific studies. However, the reported accuracies resulted from these virtual studies, that is, in the left column of Figure 4, can be under the errors encountered in MRI guided interventions due to image pixel size, as well as errors in segmentation and registration.[10,12,14,19] While the accuracy metrics are meaningful in comparing the two interfaces, their absolute numerical values relate to spatial resolution images and conditions. In these studies, the generated interventional scenes were based on phantom MR images collected with a pixel size of 0.625 × 0.625 mm. While this is a finer resolution than many studies,[10,12,14,19] studies with manipulators use finer pixel sizes with MRI, especially at higher field scanners such as 0.9 mm.[42]

The generic design of the manipulator for these studies was inspired by previous works.[15–17] In these manipulators, the actuations comprise of a set of translation and rotation motions to position a probe inside the rectum; this probe is then used to guide a biopsy needle to the targeted lesion. In our studies, the in-house developed software system was especially tuned to simulate a two rotational degrees-of-freedom transrectal manipulator that carries and positions the needle-like instrument. This is a rather generic kinematic structure encountered in most distal ends of transrectal systems. It is noted that the underlying code can be configured to replicate and simulate any manipulator by entering the appropriate kinematic solutions of the studied manipulator and adding the corresponding joint controls.

In the current studies, 2D/3D scenes of the software were rendered on an LCD screen and no additional cues for planning were provided to the operator. Future user studies will focus on investigating emerging techniques for interfacing the operator with the 3D imaging data to enhance image-guided interventions. Specifically, we consider assessing the practical value of including visual and force-feedback cues in the interface for interactively constraining the motion of an interventional probe to avoid injury to vital or healthy tissue, as demonstrated before.[43–45] Moreover, our team is currently pursuing the incorporation of holographic interfaces for immersive visualization of multimodal data;[46,47] and upon completion of its development, we will pursue additional user studies.

## 5 | CONCLUSIONS

This study describes a transrectal MR-guided prostate biopsy planning software and reports outcomes from end-user (urologists) studies. As the software acts as an interface between the operator and the biopsy system, the operator's ability to perform an accurate and safe biopsy depends crucially on the information rendered in the environment generated by the intervention planning software. These studies demonstrated that conventional 2D visualization of imaging data is more intuitive for urologists as compared to 3D, although it has limitations for certain modes of operation. Urologists with experience in 3D environments performed considerably better, independently of the urologist's medical experience. Ultimately, the results contrast 2D versus 3D visualization environments under different operational modes (side-firing or end-firing) of a biopsy system. These insights can be used for designing different features of an interventional planning software.

## ACKNOWLEDGEMENTS

This work was supported by NPRP award (NPRP 9-300-2-132) from the Qatar National Research Fund (a member of The Qatar Foundation) and by the National Science Foundation awards CNS-1646 566, DGE-1746 046, and DGE-1433 817. All opinions, findings, conclusions or recommendations expressed in this work are those of the authors and do not necessarily reflect the views of our sponsors.

## CONFLICT OF INTEREST

The authors of this submission have NO affiliations with or involvement in any organization or entity with any financial interest (such as honoraria; educational grants; participation in speakers' bureaus; membership, employment, consultancies, stock ownership, or other equity interest; and expert testimony or patent-licensing arrangements), or non-financial interest (such as personal or professional relationships, affiliations, knowledge or beliefs) in the subject matter or materials discussed in this manuscript.

## ORCID

*Jose D. Velazco-Garcia* https://orcid.org/0000-0002-1938-6770
*Nikolaos V. Tsekos* https://orcid.org/0000-0002-4327-9895

## REFERENCES

1. Wang G, Zhao D, Spring DJ, Depinho RA. Genetics and biology of prostate cancer. *Genes Dev*. 2018;32(17-18):1105-1140. https://doi.org/10.1101/gad.315739.118.
2. Siegel RL, Miller KD, Jemal A. Cancer statistics. *CA Cancer J Clin*. 2017;67(1):7-30. https://doi.org/10.3322/caac.21387.
3. Catalona WJ. Prostate cancer screening. *Med Clin North Am*. 2018;102(2):199-214. https://doi.org/10.1016/j.mcna.2017.11.001.
4. Qaseem A, Barry MJ, Denberg TD, Owens DK, Shekelle P. Screening for prostate cancer: a guidance statement from the clinical guidelines committee of the American College of Physicians. *Ann Intern Med*. 2013;158(10):761-770. https://doi.org/10.7326/0003-4819-158-10-201305210-00633.
5. Ching CB, Moussa AS, Li J, Lane BR, Zippe C, Jones JS. Does transrectal ultrasound probe configuration really matter? End fire versus side fire probe prostate cancer detection rates. *J Urol*. 2009;181(5):2077-2083. https://doi.org/10.1016/j.juro.2009.01.035.
6. Paul R, Korzinek C, Necknig U, et al. Influence of transrectal ultrasound probe on prostate cancer detection in transrectal ultrasound-guided sextant biopsy of prostate. *Urology*. 2004;64(3):532-536. https://doi.org/10.1016/j.urology.2004.04.005.
7. Moussa AS, El-Shafei A, Diaz E, et al. Identification of the variables associated with pain during transrectal ultrasonography-guided prostate biopsy in the Era of Periprostatic nerve block: the role of transrectal probe configuration. *BJU Int*. 2013;111(8):1281-1286. https://doi.org/10.1111/j.1464-410X.2012.11689.x.
8. Raber M, Scattoni V, Gallina A, et al. Does the transrectal ultrasound probe influence prostate cancer detection in patients undergoing an

extended prostate biopsy scheme? Results of a large retrospective study. *BJU Int*. 2012;109(5):672-677. https://doi.org/10.1111/j.1464-410X.2011.10522.x.
9. Rom M, Pycha A, Wiunig C, et al. Prospective randomized multicenter study comparing prostate cancer detection rates of end-fire and side-fire transrectal ultrasound probe configuration. *Urology*. 2012;80(1):15-18. https://doi.org/10.1016/j.urology.2012.01.061.
10. Verma S, Choyke PL, Eberhardt SC, et al. The current state of MR imaging–targeted biopsy techniques for detection of prostate cancer. *Radiology*. 2017;285(2):343-356. https://doi.org/10.1148/radiol.2017161684.
11. Marks L, Le J, Huang J. Targeted prostate biopsy: value of multiparametric magnetic resonance imaging in detection of localized cancer. *Asian J Androl*. 2014;16(4):529. https://doi.org/10.4103/1008-682X.122864.
12. Xu S, Kruecker J, Turkbey B, et al. Real-time MRI-TRUS fusion for guidance of targeted prostate biopsies. *Comput Aided Surg*. 2008;13(5):255-264. https://doi.org/10.3109/10929080802364645.
13. Soteria Medical. http://www.soteria-medical.com/. Accessed January 17, 2020.
14. Schouten MG, Bomers JGR, Yakar D, et al. Evaluation of a robotic technique for transrectal MRI-guided prostate biopsies. *Eur Radiol*. 2012;22(2):476-483. https://doi.org/10.1007/s00330-011-2259-3.
15. Stoianovici D, Kim C, Srimathveeravalli G, et al. MRI-safe robot for endorectal prostate biopsy. *IEEE/ASME Trans Mechatronics*. 2013;19(4):1289-1299. https://doi.org/10.1109/TMECH.2013.2279775.
16. Krieger A, Song SE, Cho NB, et al. Development and evaluation of an actuated MRI-compatible robotic system for MRI-guided prostate intervention. *IEEE ASME Trans Mechatron*. 2012;18(1):273-284. https://doi.org/10.1109/tmech.2011.2163523.
17. Krieger A, Susil R, Menard C, et al. Design of a novel MRI compatible manipulator for image guided prostate interventions. *IEEE Trans Biomed Eng*. 2005;52(2):306-313. https://doi.org/10.1109/TBME.2004.840497.
18. Yakar D, Schouten MG, Bosboom DGH, Barentsz JO, Scheenen TWJ, Fütterer JJ. Feasibility of a pneumatically actuated MR-compatible robot for transrectal prostate biopsy guidance. *Radiology*. 2011;260(1):241-247. https://doi.org/10.1148/radiol.11101106.
19. Susil RC, Ménard C, Krieger A, et al. Transrectal prostate biopsy and fiducial marker placement in a standard 1.5T magnetic resonance imaging scanner. *J Urol*. 2006;175(1):113-120. https://doi.org/10.1016/S0022-5347(05)00065-0.
20. Hata N, Jinzaki M, Kacher D, et al. MR imaging-guided prostate biopsy with surgical navigation software: device validation and feasibility. *Radiology*. 2001;220(1):263-268. https://doi.org/10.1148/radiology.220.1.r01jl44263.
21. Tewes S, Hueper K, Hartung D, et al. Targeted MRI/TRUS fusion-guided biopsy in men with previous prostate biopsies using a novel registration software and multiparametric MRI PI-RADS scores: first results. *World J Urol*. 2015;33(11):1707-1714. https://doi.org/10.1007/s00345-015-1525-4.
22. Bomers JGR, Bosboom DGH, Tigelaar GH, Sabisch J, Fütterer JJ, Yakar D. Feasibility of a 2nd generation MR-compatible manipulator for transrectal prostate biopsy guidance. *Eur Radiol*. 2017;27(4):1776-1782. https://doi.org/10.1007/s00330-016-4504-2.
23. Tokuda J, Fischer GS, DiMaio SP, et al. Integrated navigation and control software system for MRI-guided robotic prostate interventions. *Comput Med Imaging Graph*. 2010;34(1):3-8. https://doi.org/10.1016/j.compmedimag.2009.07.004.
24. Velazco-Garcia JD, Navkar NV, Balakrishnan S, et al. Preliminary evaluation of robotic transrectal biopsy system on an interventional planning software. Proceedings - 2019 IEEE 19th International Conference on Bioinformatics and Bioengineering, BIBE 2019. IEEE; 2019.
25. Velazco-Garcia JD, Velasquez C, Balakrishnan S, et al. A generic cable-driven manipulator for targeted transrectal MR-guided prostate biopsy: Preliminary design and intervention planning. CARS 2019—Computer Assisted Radiology and Surgery Proceedings of the 33rd International Congress and Exhibition. Vol 14. Rennes, France: NLM (Medline); 2019:S144-S146. https://doi.org/10.1007/s11548-019-01969-3.
26. Velazco Garcia JD, Navkar NV, Gui D, et al. A platform integrating acquisition, reconstruction, visualization, and manipulator control modules for MRI-guided interventions. *J Digit Imaging*. 2019;32-(3):420-432. https://doi.org/10.1007/s10278-018-0152-1.
27. The Qt Company. Qt | cross-platform software development for embedded and desktop. 2019. https://www.qt.io. Accessed July 23, 2019.
28. Kitware. VTK—the visualization toolkit. 2019. https://www.vtk.org/. Accessed July 23, 2019.
29. Zamecnik P, Schouten MG, Krafft AJ, et al. Automated real-time needle-guide tracking for fast 3-T MR-guided transrectal prostate biopsy: a feasibility study. *Radiology*. 2014;273(3):879-886. https://doi.org/10.1148/radiol.14132067.
30. Halstuch D, Baniel J, Lifshitz D, Sela S, Ber Y, Margel D. Assessment of needle tip deflection during transrectal guided prostate biopsy: implications for targeted biopsies. *J Endourol*. 2018;32(3):252-256. https://doi.org/10.1089/end.2017.0694.
31. Stone NN, Mouraviev V, Schechter D, et al. Deflection analysis of different needle designs for prostate biopsy and focal therapy. *Technol Cancer Res Treat*. 2017;16(5):654-661. https://doi.org/10.1177/1533034616671007.
32. Park YL, Elayaperumal S, Daniel B, et al. Real-time estimation of 3-D needle shape and deflection for MRI-guided interventions. *IEEE/ASME Trans Mechatronics*. 2010;15(6):906-915. https://doi.org/10.1109/TMECH.2010.2080360.
33. Moreira P, Boskma KJ, Misra S. Towards MRI-guided flexible needle steering using fiber bragg grating-based tip tracking. Proceedings - IEEE International Conference on Robotics and Automation. Institute of Electrical and Electronics Engineers Inc.; 2017:4849-4854. https://doi.org/10.1109/ICRA.2017.7989564.
34. Moreira P, van de Steeg G, Krabben T, et al. The MIRIAM robot: a novel robotic system for MR-guided needle insertion in the prostate. *J Med Robot Res*. 2017;02(04):1750006. https://doi.org/10.1142/s2424905x17500064.
35. Venugopal N, McCurdy B, Hnatov A, Dubey A. A feasibility study to investigate the use of thin-plate splines to account for prostate deformation. *Phys Med Biol*. 2005;50(12):2871-2885. https://doi.org/10.1088/0031-9155/50/12/010.
36. Oguro S, Tokuda J, Elhawary H, et al. MRI signal intensity based B-spline nonrigid registration for pre- and intraoperative imaging during prostate brachytherapy. *J Magn Reson Imaging*. 2009;30(5):1052-1058. https://doi.org/10.1002/jmri.21955.
37. Fei B, Duerk JL, Wilson DL. Automatic 3D registration for interventional MRI-guided treatment of prostate cancer. *Comput Aided Surg*. 2002;7(5):257-267. https://doi.org/10.1002/igs.10052.
38. Du Bois D'Aische A, De Craene M, Haker S, et al. Improved non-rigid registration of prostate MRI. Lecture Notes in Computer Science. Vol 3216. Springer Verlag; 2004:845-852. https://doi.org/10.1007/978-3-540-30135-6_103.
39. Bharatha A, Hirose M, Hata N, et al. Evaluation of three-dimensional finite element-based deformable registration of pre- and intraoperative prostate imaging. *Med Phys*. 2001;28(12):2551-2560. https://doi.org/10.1118/1.1414009.
40. Risholm P, Fedorov A, Pursley J, Tuncali K, Cormack R, Wells WM. Probabilistic non-rigid registration of prostate images: modeling and quantifying uncertainty. Proceedings-International Symposium on

Biomedical Imaging. Vol 2011. NIH Public Access; 2011:553-556. https://doi.org/10.1109/ISBI.2011.5872467.

41. De Silva T, Fenster A, Bax J, et al. Quantification of prostate deformation due to needle insertion during trus-guided biopsy: Comparison of hand-held and mechanically stabilized systems. *Med Phys*. 2011;38(3):1718-1731. https://doi.org/10.1118/1.3557883.
42. Zangos S, Melzer A, Eichler K, et al. MR-compatible assistance system for biopsy in a high-field-strength system: initial results in patients with suspicious prostate lesions. *Radiology*. 2011;259(3):903-910. https://doi.org/10.1148/radiol.11101559.
43. Navkar NV, Deng Z, Shah DJ, Bekris KE, Tsekos NV. Visual and force-feedback guidance for robot-assisted interventions in the beating heart with real-time MRI. Proceedings - IEEE International Conference on Robotics and Automation. Institute of Electrical and Electronics Engineers Inc.; 2012:689-694. https://doi.org/10.1109/ICRA.2012.6224582.
44. Navkar NV, Deng Z, Shah DJ, Tsekos NV. A framework for integrating real-time MRI with robot control: application to simulated transapical cardiac interventions. *IEEE Trans Biomed Eng*. 2013;60(4):1023-1033. https://doi.org/10.1109/TBME.2012.2230398.
45. Navkar NV, Yeniaras E, Shah DJ, Tsekos NV, Deng Z. Generation of 4D access corridors from real-time multislice MRI for guiding transapical aortic valvuloplasties. Lecture Notes in Computer Science (Including Subseries Lecture Notes in Artificial Intelligence and Lecture Notes in Bioinformatics). Vol. 6891. LNCS; 2011:251-258. https://doi.org/10.1007/978-3-642-23623-5_32.
46. Morales Mojica CM, Navkar NV, Tsekos NV, Webb A, Birbilis T, Seimenis I. Holographic interface for three-dimensional visualization of MRI on holoLens: a Prototype platform for MRI guided neurosurgeries. Proceedings - 2017 IEEE 17th International Conference on Bioinformatics and Bioengineering. BIBE; 2017:2017. https://doi.org/10.1109/BIBE.2017.00-84.
47. Mojica CMM, Velazco-Garcia JD, Navkar NV, et al. A prototype holographic augmented reality interface for image-guided prostate cancer interventions. In Proceedings of Eurographics Workshop on Visual Computing for Biology and Medicine (EG VCBM). 2018:17-21. https://doi.org/10.2312/VCBM.20181225.

**How to cite this article:** Velazco-Garcia JD, Navkar NV, Balakrishnan S, et al. End-user evaluation of software-generated intervention planning environment for transrectal magnetic resonance-guided prostate biopsies. *Int J Med Robot*. 2021;17:e2179. https://doi.org/10.1002/rcs.2179